

## Supplementary Information

### Pt-free Microengines at Extremely Low Peroxide Levels

Heng Ye<sup>a</sup>, Guofeng Ma<sup>b</sup>, Jian Kang<sup>a</sup>, Hongqi Sun<sup>c,\*</sup>, and Shaobin Wang<sup>a,\*</sup>

<sup>a</sup> *Department of Chemical Engineering, Curtin University, GPO Box U1987, Perth, Western Australia, 6845, Australia*

<sup>b</sup> *Key Lab of Advance Materials Technology of Educational Department Liaoning Province, Shenyang University, Shenyang, 110044, China*

<sup>c</sup> *School of Engineering, Edith Cowan University, 270 Joondalup Drive, Joondalup, Western Australia, 6027, Australia*

\* *Correspondence and requests for materials should be addressed to S.W. (Email:*

*[shaobin.wang@curtin.edu.au](mailto:shaobin.wang@curtin.edu.au))*

## **Description of Videos:**

**Video S1.** Motion behaviors of graphene/FeO<sub>x</sub>-MnO<sub>2</sub> microtube micromotors in 0.03% H<sub>2</sub>O<sub>2</sub>, showing small circular motion.

**Video S2.** Motion behaviors of graphene/FeO<sub>x</sub>-MnO<sub>2</sub> microtube micromotors in 0.3% H<sub>2</sub>O<sub>2</sub> showing helical motion behaviors.

**Video S3.** Motion behaviors of graphene/FeO<sub>x</sub>-MnO<sub>2</sub> microtube micromotors in 3% H<sub>2</sub>O<sub>2</sub> showing ultra-fast irregular motion.

## **EXPERIMENTAL SECTION**

### **Materials and reagents**

Potassium permanganate, iron (III) nitrate, sodium sulfate, ethanol, dichloromethane, sodium dodecyl sulfate (SDS), and sulfate acid (98%) were purchased from Sigma-Aldrich. Hydrogen peroxide (30%) was purchased from ROWE Scientific Australia. Aluminum oxide paste was purchased from Kemet, NSW, Australia. Porous polycarbonate (PC) membranes with an average pore diameter of 5 μm were purchased from Whatman Inc., NY, USA. Ultrapure water (milli-Q) was used in all experiments. Nano-sized graphene oxide (GO) was purchased from graphene supermarket, New York, USA.

### **Fabrication of MnO<sub>2</sub> based micromotors**

Graphene/FeO<sub>x</sub>-MnO<sub>2</sub> based micromotors were fabricated using a template-assisted electrochemical deposition protocol. A cyclopore polycarbonate membrane containing 5 μm conical-shaped micropores (Whatman, NY, USA) was employed as the template. An 80 nm of gold film was first deposited on one side of the porous membranes to serve as the working electrode using an Emitech K950X gold evaporator and performed at room temperature under a high vacuum of below 1×10<sup>-3</sup> mbar at a direct current of 6 A. The deposition rate was about 1 nm s<sup>-1</sup>. A customized plating cell was used in all electrochemical deposition processes. The membrane was assembled in a self-designed plating cell with an aluminum foil serving as the

contact for the working electrode. Electrochemical deposition was carried out using an electrochemical workstation (Zennium Zahner, Germany). A Pt wire and Ag/AgCl with 3M KCl were used as the counter and reference electrodes, respectively. A mixed solution of 0.1 mg mL<sup>-1</sup> nano-sized graphene oxide in 0.5 M of Na<sub>2</sub>SO<sub>4</sub> and 0.1 M H<sub>2</sub>SO<sub>4</sub> was prepared as the electrolyte for the electrochemical growth of graphene outer layer. The graphene oxide in the solution was reduced by a cyclic voltammetry (CV) method from 0.3 to -1.5 V for five cycles. After washing with 10 mL of ultrapure water for three times, the inner FeO<sub>x</sub>-MnO<sub>2</sub> catalyst were deposited using a galvanostatic (GS) method at a current of -3 mA for 10 and 30min, respectively, which equals to 1.8 C and 5.4 C of charge transferred. Galvanostatic deposition at -3 mA for 10 min results in the formation of tubular shaped micromotors. Galvanostatic deposition at -3 mA for 30 min results in the total closure of the microtubes, forming the graphene wrapped microrods architecture. The electrolyte contains 20 mM of Fe(NO<sub>3</sub>)<sub>3</sub> and 20 mM KMnO<sub>4</sub>. Following the electroreduction deposition, the gold layer was removed by hand polishing with alumina slurry. Then the templates were dissolved in dichloromethane for 15 min to release the micromotors. Finally, the micromotors were collected by centrifugation at 7000 rpm for 3 min while being repeatedly washed with dichloromethane, ethanol and ultrapure water for three times each. The ultrasonication process was carried out using a Unisonics ultrasonication cleaner (Model FXP12D), and the centrifugation was carried out using an Eppendorf centrifuge 5430. All the micromotors were stored in ultrapure water at room temperature for further use.

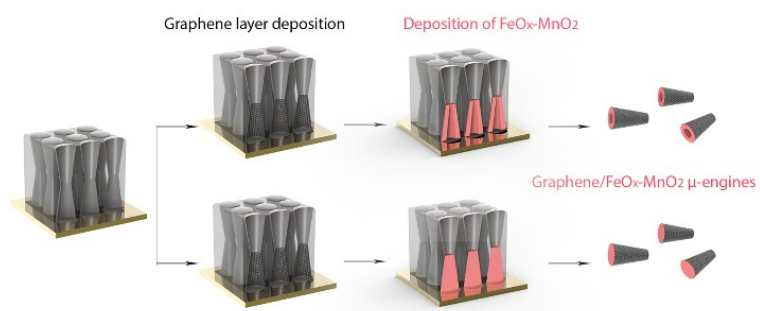
### **Characterization of the micromotors.**

Scanning electronic microscopy (SEM/EDS) analysis was conducted using a Zeiss 1555 VP-FESEM with a field emission electron gun and the Oxford EDS detector operated by the Aztec software. SEM images were taken at the acceleration voltages from 2 to 5 kV. EDS analysis was taken using the coupled Oxford detector of the microscope and operated by the Aztec software at an acceleration voltage of 15 kV. X-ray photoelectron spectroscopy (XPS) was

carried out on a thermos ESCALAB 250 XPS microscope with monochromatic Al-K $\alpha$  X-rays at a photo energy of 1486.7 eV. The measurement was carried out using a Kratos AXIS Ultra DLD system under UHV conditions with a base pressure less than  $1 \times 10^{-9}$  mBar. The spectra were acquired with the pass energy of 20 eV and fitted using CasaXPS software. All spectra were calibrated to yield a primary C 1s component at 284.6 eV with the Shirley background, and the component fitting was applied by Voigt functions with 30% Lorentzian component.

### **Motion behavior observation.**

A transparent plastic petri dish (Part No. P35G-1.5-10-C, Mat Tek Corporation, MA, USA) with holed bottom covered by a thin glass slide was used as the container to prepare different fuel concentrations for the observation of motion behaviors. A 10 mm diameter bottom hole of the 35 mm diameter plastic petri dish was covered by a thin glass slide, which formed a shallow well-like hollow structure with a volume of approximately 75-80  $\mu$ L. SDS was used as the surfactant for motion behavior observation in all experiments. Optical microscopy videos and images were obtained using an Olympus IX81 inverted microscope with a Nikon digital sight DS-2Mv camera connected to a computer and operated by the Nikon NIS-Elements software. Motion videos were recorded at about 12.5 frames per second using a 4X objective. The time interval between two frames are 0.08 s. Free Fiji software was used to calculate the speed of micromotors, edit videos and extract pictures. A digital hand-held "Pocket" H<sub>2</sub>O<sub>2</sub> refractometer (Model: Atago, PAL-39S) was used to calibrate the concentrations of H<sub>2</sub>O<sub>2</sub> solutions.



**Scheme S1** Schematic illustration of the fabrication process of the graphene/FeO<sub>x</sub>-MnO<sub>2</sub> based micromotors.

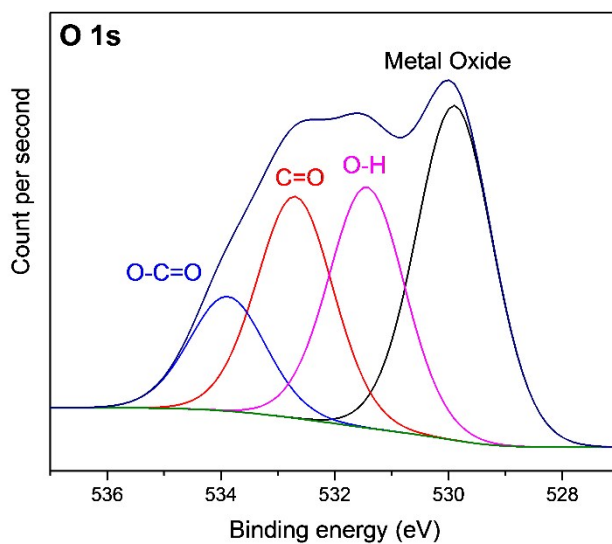


**Fig. S1** XPS results of the O1s spectra of the erGO/FeO<sub>x</sub>-MnO<sub>2</sub> micromotors.

**Table S1** Various functional groups identified on the surface of erGO/FeO<sub>x</sub>-MnO<sub>2</sub> micromotors.

Spectra	Group	Position (eV)	at. %
C 1s	C-C/C-H/C=C	284.6	68.33
C 1s	C-O	286.26	20.41
C 1s	C=O	288.40	6.47
C 1s	O-C=O	290.28	4.79
O 1s	Metal Oxide	529.89	36.71
O 1s	O-H	531.44	26.41
O 1s	C=O	532.70	24.32
O 1s	O-C=O	533.88	12.57

**Table S2** Comparison of the performance of catalytic micro/nanomotors.

Type of the micro-/nanomotor	Ref.	Size [ $\mu\text{m}$ ]	Fuel concentration range ( $\text{H}_2\text{O}_2$ )	Average speed [ $\mu\text{m s}^{-1}$ ]	Max. speed reported [ $\mu\text{m s}^{-1}$ ]	Max. relative speed (bl $\text{s}^{-1}$ )	Efficiency or propelling force (pN)
Rolled up Ti/Cr/Pt microtubes	Sanchez and Schmidt et al. <sup>1</sup>	50	0.25-5% (v/v)	140-10000 at 37°C	10000	200	
Multilayered microrockets	Li and Zhang et al. <sup>2</sup>	20	1-5%	285-1410	1410	70	
Pt-Alloy nanowires	Wang et al. <sup>3</sup>	2	15%	110	160	75	
Au/Pt-CNT nanowires	Wang et al. <sup>4</sup>	2	15%	51	91	45.5	
Cu/Pt concentric bimetallic microtubes	Zhao and Pumera et al. <sup>5</sup>	10	0.2-3%	70-700	n.a.	70	
Cu/Ag segmented bimetallic tubular micromotors	Pumera et al. <sup>6</sup>	10-15	0.5-3%	13.1-252.4	n.a.	n.a.	$2.52 \times 10^{-9}$
Ag and $\text{MnO}_2$ microparticles	Pumera et al. <sup>7</sup>	Ag $\approx$ 30 $\text{MnO}_2 \approx$ 5	0.1-12% 12-21%	25-100 50-120	n.a.	n.a.	$5.81 \times 10^{-8}$ $1.16 \times 10^{-8}$
Au/Graphene/ $\text{MnO}_2$	Feng and Ma et al. <sup>8</sup>	6.74	0.15-2.5%	15.79-44.79	111.03	27.69	
PEDOT/ $\text{MnO}_2$ microtubes & microrods And $\text{MnO}_2 @ \text{MnCO}_3$	Saldar and Janis et al. <sup>9</sup>	12.5 12.5 5	5-15 5-15 1-10	Tubes 200-510 Rods 200-410 142-665	n.a. 900	n.a. 180	
Graphene/Pt	Wang et al. <sup>10</sup>	10	0.1-3	37-1700	n.a.	170	
$\text{MnO}_2$ hallow	Saldar and Janis et al. <sup>11</sup>	n.a.	5-10	321-996	1625	n.a.	
PANI/Pt microtubes	Gao and Wang et al. <sup>12</sup>	8	0.2-5	25-1410	3000	375	45 pN
PEDOT/Pt bilayer microtubes PPy/Ag bilayer PPy/Pt-Ni alloy Au/Pt bimetallic microbots	Gao and Wang et al. <sup>13</sup>	7	10 5-10 15 10 10	10000 at 37°C 2400-3350 500 470 1500	10000 at 37°C 3375 at 20°C	1400 480 70 67	
Paper tubular microjet engines	Singh and Mandal et al. <sup>14</sup>	900	9-16	270-1600	1600	2	
PEDOT/ $\text{MnO}_2$	Wang et al. <sup>15</sup>	8	0.4-10	31.57-318.80	n.a.	n.a.	
PEDOT/PtNP@CNT-PPy	Li and Wu et al. <sup>16</sup>	12	1-15	62-450	n.a.	n.a.	10 pN
Porous Ti/Cr/Pt microtubes	Mei et al. <sup>17</sup>	10-40	0.2-7	120-1077	>1500	n.a.	
erGO/ $\text{MnO}_2$ microtubes by anodic deposition	Our previous work <sup>18</sup>	8	3-15	77-466	700	87.5	36 pN
erGO/ $\text{FeO}_x$ - $\text{MnO}_2$ microtubes	This work	12	0.03-5%	89-1279	1779	148.25	6-91 pN

Upon fuel addition, microbubbles were generated and the micromotors start to move. The lifetime of these micromotors could exceed 25 min but only the first few minutes were taken into account for the speed calculation as fuel depletion will have a significant effect on the mobility of micromotors. At a very high content of fuels, such as 10% of H<sub>2</sub>O<sub>2</sub>, the fuel solution reacts very fast with the catalytic micromotors, thus the observed lifetime of micromotors is shortened due to the consumption of the catalytic materials. At a very low content of fuel, such as 0.03% H<sub>2</sub>O<sub>2</sub>, although the reaction consumption of catalytic materials is not a problem, the fuel depletion will significantly affect the lifetime of these micromotors, and these micromotors will stop moving very soon. Upon refuelling the petri dish, these micromotors will initiate motion again. We have observed that, at moderate fuel levels and surfactant content, these micromotors can navigate for more than 25 min in one test.

Taking the microengines as a cylinder microrod, we can adopt the Stokes' drag theory to estimate the drag force or propelling force roughly by the following equation.<sup>12, 16</sup>

$$F_d = \frac{2\pi\mu LU}{\ln(L/a) - 1/2} \quad (1)$$

Where  $F_d$  is the fluid resistance,  $U$  is the speed of the microengines,  $\mu$  is the fluid dynamic viscosity, and  $L$  and  $a$  are the length and radius of the micromotors, respectively. The estimated drag forces for the four types of micromotors are presented in Table S3, which also summarizes the speed profile of different MNMs reported so far. The estimated drag force for the graphene/FeO<sub>x</sub>-MnO<sub>2</sub> micromotors are 6.3 pN in 0.03% H<sub>2</sub>O<sub>2</sub> and 91.1 pN in 5% H<sub>2</sub>O<sub>2</sub>.

## References

- 1 S. Sanchez, A. N. Ananth, V. M. Fomin, M. Viehrig and O. G. Schmidt, *J. Am. Chem. Soc.*, 2011, **133**, 14860-14863.



- 2 T. L. Li, L. Q. Li, W. P. Song, L. Wang, G. B. Shao and G. Y. Zhang, *ECS J. Solid State Sci. Technol.*, 2015, **4**, S3016-S3019.
- 3 U. K. Demirok, R. Laocharoensuk, K. M. Manesh and J. Wang, *Angew. Chem. Int. Ed.*, 2008, **47**, 9349-9351.
- 4 R. Laocharoensuk, J. Burdick and J. Wang, *ACS Nano*, 2008, **2**, 1069-1075.
- 5 G. J. Zhao and M. Pumera, *RSC Adv.*, 2013, **3**, 3963-3966.
- 6 W. Z. Teo, H. Wang and M. Pumera, *Chem. Commun.*, 2016, **52**, 4333-4336.
- 7 H. Wang, G. J. Zhao and M. Pumera, *J. Am. Chem. Soc.*, 2014, **136**, 2719-2722.
- 8 X. M. Feng, Y. Zhang, Y. Li, Z. D. Huang, S. F. Chen, Y. W. Ma, L. Zhang, L. H. Wang and X. H. Yan, *Chem. Lett.*, 2015, **44**, 399-401.
- 9 M. Safdar, O. M. Wani and J. Janis, *ACS Appl. Mater. Interface*, 2015, **7**, 25580-25585.
- 10 A. Martin, B. Jurado-Sanchez, A. Escarpa and J. Wang, *Small*, 2015, **11**, 3568-3574.
- 11 M. Safdar, T. D. Minh, N. Kinnunen and J. Janis, *ACS Appl. Mater. Interface*, 2016, **8**, 32624-32629.
- 12 W. Gao, S. Sattayasamitsathit, J. Orozco and J. Wang, *J. Am. Chem. Soc.*, 2011, **133**, 11862-11864.
- 13 W. Gao, S. Sattayasamitsathit, A. Uygun, A. Pei, A. Ponedal and J. Wang, *Nanoscale*, 2012, **4**, 2447-2453.
- 14 A. K. Singh, T. K. Mandal and D. Bandyopadhyay, *RSC Adv.*, 2015, **5**, 64444-64449.
- 15 L. L. Wang, J. Chen, X. M. Feng, W. J. Zeng, R. Q. Liu, X. J. Lin, Y. W. Ma and L. H. Wang, *RSC Adv.*, 2016, **6**, 65624-65630.
- 16 Y. N. Li, J. Wu, Y. Z. Xie and H. X. Ju, *Chem. Commun.*, 2015, **51**, 6325-6328.
- 17 J. X. Li, Z. Q. Liu, G. S. Huang, Z. H. An, G. Chen, J. Zhang, M. L. Li, R. Liu and Y. F. Mei, *NPG Asia Mater.*, 2014, **6**, e94.
- 18 H. Ye, H. Q. Sun and S. B. Wang, *Chem. Eng. J.*, 2017, **324**, 251-258.